Dramatic enhancement of capillary wave fluctuations of a decorated water surface

A. Datta, S. Kundu, and M. K. Sanyal
Surface Physics Division, Saha Institute of Nuclear Physics, Kolkata 700064, India

J. Daillant, D. Luzet, and C. Blot
LIONS, Service de Chimie Moléculaire, bât. 125, CEA Saclay, F-91191 Gif-sur-Yvette Cedex, France

B. Struth
European Synchrotron Radiation Facility, B.P. 220, F-38043 Grenoble Cedex, France
(Received 22 September 2004; revised manuscript received 8 December 2004; published 8 April 2005)

We have demonstrated by x-ray diffuse scattering that a *bimolecular layer* of a preformed three-tailed amphiphile, ferric stearate, drastically enhances capillary wave fluctuations on water surface due to a reduction in surface tension to 1 mN/m. The bimolecular layer is composed of molecules in symmetric configuration, on top of molecules in asymmetric configuration with ferric ions in contact with water. Unlike the usual Langmuir monolayers, this layer of molecules does not rupture under compression, but becomes thicker. This behavior mimics folding of a membrane on a liquid surface and is closely related to the cohesive interaction brought by the ferric ions. The low *effective tension* of this artificial membrane depends on the available area and reduces as the microscopic excess area increases.

DOI: 10.1103/PhysRevE.71.041604 PACS number(s): 68.03.Cd, 61.10.Kw, 68.18.−g

I. INTRODUCTION

Among the anomalous properties of water one is its large surface tension, the work required to increase a surface by unit area: $\gamma_{\text{water}}=73$ mN/m at room temperature. Surface tension is known to arise from uncompensated interactions at the surface. More specifically, using the so-called mechanical definition of surface tension [1], $\gamma=\int dz(\pi_{\perp}-\pi_{\parallel})$, the surface tension can be expressed as the difference between the normal $\pi_{\perp}$ (constant) and parallel $\pi_{\parallel}$ components of the nonisotropic pressure tensor across the interface. Except for critical interfaces with smooth interfacial gradients, very low interfacial tension values ≈ 1 μN/m are only achieved in microemulsions [2,3] and lipid membranes. A microemulsion water-oil interface is indeed saturated with surfactant, and in the above formalism, repulsion in the chain region compensates for the attraction at the hydrophobic-water interface which can be described using an effective surface energy ≈ 20 mN/m [4].

Surface tension controls fluctuations and, therefore, interfacial morphology. The water surface is extremely flat, its rms roughness being of the order of 0.5 nm, due to the large tension (and not gravity for distances below the capillary length ≈ 2.7 mm) [5–8]. On the other hand, microemulsion interfaces, membranes, or vesicles are heavily fluctuating surfaces. In such cases when a low enough surface tension is reached, entropic (fluctuation-related) contributions to the surface tension are no longer negligible [9–11]. This is, for example, the case in vesicles, where the bilayer tension can be measured in a micropipette experiment [12]. In this communication, we show that a layer of preformed ferric stearate can be tailored in such a way as to decrease the surface tension of the water subphase down to 1 mN/m, more than one order of magnitude below the value (≈ 20 mN/m) obtained with standard surfactants. As a result, the surface fluctuations, which we are probing from nanometer to micrometer length scale using diffuse x-ray scattering measurements [13,14], are strongly enhanced.

II. PREFORMED FERRIC STEARATE

A. Motivation

Fluctuations and structures of Langmuir monolayers of fatty-acid salts of multivalent metals have been studied extensively [15,16]. The standard way of studying them is to have the Langmuir monolayer of the *fatty-acid* spread on the surface of water containing *ions of the relevant metal*, and for divalent metals it has been shown that about one hydrocarbon chain of the fatty acid is associated with one metal ion [17] [Fig. 1, inset (a)]. However, in this method the number of metal ions and the number of acid molecules available are far from equal and this introduces a large uncertainty in the composition of the monolayer of a multivalent-metal salt. On the other hand, if a salt of a long-chain fatty acid is formed beforehand through chemical reaction and a monolayer of this *preformed salt* is spread on water, the head-to-tail ratio of amphiphiles in the monolayer is fixed. But for such preformed salts of multivalent metals, even the molecular configuration at the air-water interface is unknown, to the best of our knowledge.

Ferric salts of amphiphilic fatty acids are amphiphilic molecules with three hydrocarbon chains. Of these salts the best known is ferric stearate (FeSt), given by the chemical formula of $Fe[OOC(CH_2)_{16}CH_3]_3$ bearing three hydrocarbon chains. This salt is easy to prepare and purify, and has many practical uses. Langmuir monolayers of FeSt have been studied through surface-pressure specific-molecular-area (π-A) isotherms where the surface pressure π is defined as $\pi=\gamma_{\text{water}}-\gamma$, γ being the surface tension of monolayer-covered

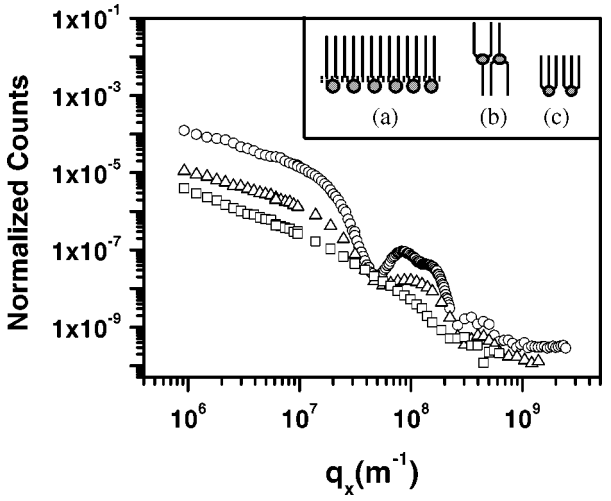

FIG. 1. X-ray scattering in the vertical plane of incidence—i.e., low-$q_{\|}$ scattering ($\psi=0$) from the water surface (open squares)—from film of stearic acid at surface pressure of 20 mN/m over millimolar aqueous solution of ferric chloride (open triangles) and from film of ferric stearate at the same surface pressure over water (open circles). Inset: model of (a) stearic acid molecules in a film over metal ions in water, (b) pair of ferric stearic molecules in the "symmetric" Y and inverted-Y conformation, and (c) pair of ferric stearate molecules in the "asymmetric" conformation.

water [18,19]. Langmuir-Blodgett (LB) films of FeSt have been used as templates for synthesis of two-dimensional organic semiconductors [20], of magnetic multilayers [21], and as two-dimensional magnets as such [22].

In our previous studies we have observed that surface densities are anomalously high in films of preformed FeSt at air-water interfaces [19] and a "constant-pressure collapse" of the film occurs at very high surface pressure—i.e., very low surface tension. We have also observed that there is no surface energy change during formation of LB films of FeSt from such films [23]. These results cannot be reconciled with the preformed ferric stearate undergoing dissociation at water surface to produce the situation depicted in Fig. 1 [inset (a)]. To explain the anomalous surface density of FeSt film on water a "symmetric" conformation of FeSt molecules in the film was involved. This conformation consists of an adjacent pair of FeSt molecules in the "Y and inverted-Y" configurations, as shown in Fig. 1 [inset (b)] with one (two) chains below and the other two (one) chains above the Fe-bearing head group. Both individual molecules, as well as the pair, has very small dipole moment in this configuration, and it was suggested that such pairs build up the film of FeSt on water. Though the symmetric conformation could explain the surface density anomaly observed [19], the large repulsion between hydrocarbon and water does not tally with the observed stability of the film. On the other hand, FeSt molecules in the asymmetric conformation, shown in Fig. 1 [inset (c)], has the Fe-bearing head group below all three hydrocarbon chains. Molecules in the asymmetric conformation have a high dipole moment and due to the resulting hydrophilic interaction will be energetically stable on water surface, but they do not explain the density anomaly. It was, therefore, of considerable interest to find the actual structure of a film of preformed FeSt on water surface and to study the reduction of surface tension caused by such a stable film with a high surface density.

X-ray diffuse scattering techniques have been used extensively to measure surface tension of liquids through amplitude of capillary waves [5–8,24,25]. We have used this technique to measure the surface tension of films of preformed FeSt on water surface, at different macroscopic surface pressures (measured by a Wilhelmy plate). Scatterings of x rays in the plane of FeSt-film-covered water and in the plane normal to the water (horizontal) surface are dependent, respectively, on the in-plane and out-of-plane structures of the FeSt film. Though the main focus of the present communication is the effect of the FeSt film on reduction of surface tension and associated structure of FeSt film on water surface, for the purpose of clarity we have also presented the results of atomic force microscopy (AFM) and x-ray scattering studies of FeSt films transferred onto Si(001) substrates using a horizontal deposition technique [26].

B. Sample preparation

Ferric stearate was prepared through stepwise reactions [19]. At first sodium stearate was prepared by adding sodium hydroxide (Merck, 99%) in hot Milli-Q water (resistivity 18.2 MW cm) containing stearic acid (Sigma, 99.9%) in appropriate amounts. Sodium hydroxide was added until the medium was slightly alkaline ($p\mathrm{H}\sim 7.0-7.5$). Sodium stearate was completely soluble in hot water. Measured amount of ferric chloride (Merck, 99%) solution was then added in the freshly prepared sodium stearate solution in hot condition so the FeSt is formed and collected after filtration. As FeSt is completely insoluble in water at all temperatures, it is then washed repeatedly by hot Milli-Q water to remove unreacted sodium stearate and other water soluble impurities. It is then washed with benzene (SLR, 99.8%) to remove unreacted stearic acid and other organic impurities. Fourier transform infrared (FTIR) spectra of the purified FeSt sample were collected in the $670-4000\ \mathrm{cm}^{-1}$ range with a Spectrum GX (Perkin Elmer) spectrometer in the attenuated total reflection (ATR) mode at a resolution of $4\ \mathrm{cm}^{-1}$. The presence of strong bands corresponding to carboxylate asymmetric and symmetric stretch modes indicates a large conversion of the fatty acid to the metal-bearing salt. Very weak bonds corresponding to COOH deformation and stretch and to hydroxyl stretch indicate, respectively, very small amounts of free acid and hydroxy groups in the sample.

III. STUDIES OF FERRIC STEARATE FILMS

A. Experimental details

Ferric stearate molecules were spread from a 1.1 mg/mL chloroform solution in a homemade Langmuir trough of 800 cm^2 surface area on Milli-Q water at room temperature. 100 μl of the spreading solution was spread and the resulting monolayer was compressed at a slow rate ($1\ \mathrm{mm}^2/\mathrm{min}$). The surface pressure (π) was measured using a Wilhelmy balance with a paper Wilhelmy plate. For comparison, 100 μl of stearic acid molecules from a 1.2 mg/mL chloroform solu-

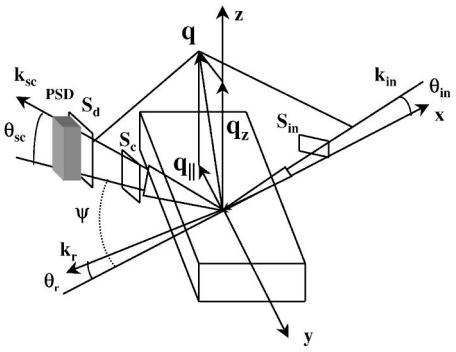

FIG. 2. Schematics of the experiment. The scattering solid angle is defined by the slits $S_{in}=300\ \mu\text{m}\times 100\ \mu\text{m}$ ($H\times V$). Two scattering geometries with two different detectors are used; for low-$q_\parallel$ scattering ψ is set to zero and the PSD is replaced by a point detector (refer text).

tion were also spread on $\simeq 10^{-4}M$ solution of ferric chloride in water. X-ray scattering experiments described in this communication were carried out at the TROIKA-II(10IDB) beamline of the European Synchrotran Research Facility (ESRF), using an 8.04-kev x-ray beam having wavelength $\lambda=0.15421$ nm. The Langmuir trough was mounted on an active antivibration system with the centre of the six-circle diffractometer of TROIKA-II lying on water surface of the trough. Experiments were performed in He atmosphere to reduce absorption and scattering by air. The incident beam was defined (Fig. 2) by the slit S_{in} ($300\ \mu\text{m}\times 100\ \mu\text{m}$) and the grazing angle of incidence θ_{in}, with the water surface, was kept at 1.87 mrad, below the critical angle θ_{sc} for total external reflection from water.

In order to record surface scattering over the widest possible range of $\mathbf{q}_\parallel=(\mathbf{q}_x,\mathbf{q}_y)$, two different scattering geometries were used by us in our experiments. The experimental details have been described elsewhere [14] and are presented schematically in Fig. 2. This figure depicts the geometry used to collect high-$q_\parallel$ data. The scattered data were collected with a vertically mounted position-sensitive detector (PSD), scanning the PSD in the plane of the surface around a vertical axis. The scattering solid angle is defined by the slits S_c (300 μm wide) and S_d (500 μm wide) at distances of 605 mm and 809 mm, respectively, from the diffractometer center. Whereas the intensity profile along the PSD is proportional to the vertical (out-of-plane) structure factor $S(q_z)$, the integrated intensity is proportional to the surface fluctuation spectrum integrated along the propagation direction x, with $q_\parallel\simeq(2\pi/\lambda)\cos\psi$ where ψ is the angle the scattered beam makes with the specular plane, along the water surface (horizontal plane). This setup was also used to perform grazing incidance diffraction (GID) measurements at large values of ψ. The scattering geometry adopted for collecting the low-$\mathbf{q}_\parallel$ part of the data was obtained by scanning a NaI scintillator or "point detector" in the vertical specular plane, i.e., at $\psi=0$. The scattered beam was defined by two slits S_u ($1.0\ \text{mm}\times 7.0\ \text{mm}$) and S_v ($0.5\ \text{mm}\times 7.0\ \text{mm}$) placed at 460 mm and 690 mm, respectively, from the diffractometer center. If the direction of the wide opening of these slits is taken to be the y direction, the collected signal is integrated over surface fluctuations in the y direction. In this geometry, thus the scattered signal is proportional to $S(q_z)$ times the surface fluctuation spectrum $S_h(q_\parallel)$ integrated along y, whence $q_\parallel=q_x\simeq(\pi/\lambda)(\theta_{in}^2-\theta_{sc}^2)$. Combining both geometries, fluctuation spectra could be determined over more than five orders of magnitude from about $10^5\ \text{m}^{-1}$ to $10^{10}\ \text{m}^{-1}$. Extreme care was taken to minimize and subtract the background, which is essential for measuring the very small surface signal, less than 10^{-11} of the incident intensity, obtained at high $q_\parallel$.

B. Analysis technique

If θ_{in} is the incident angle and θ_{sc} is the scattering angle in the vertical plane, perpendicular to the water surface, and ψ is the azimuthal angle of this vertical plane, on water surface, with respect to the specular plane ($\psi=0$, for specular plane), then the momentum transfer vector is given by its components $q_x=(2\pi/\lambda)(\cos\theta_{sc}\cos\psi-\cos\theta_{in})$, $q_y=(2\pi/\lambda)\cos\theta_{sc}\sin\psi$, and $q_z=2\pi/\lambda(\sin\theta_{sc}+\sin\theta_{in})$. For specular reflection, $q_x=q_y=0$ and $\theta_{sc}=\theta_{in}$; hence, $q_z=(4\pi/\lambda)\sin\theta_{in}$.

The total diffuse scattered x-ray intensity spectra obtained in our experiments can be expressed in terms of the differential scattering cross section for a two-component, heterogeneous [14] film:

$$\frac{d\sigma}{d\Omega}=Ar_e^2|t_{01}^{in}|^2|t_{01}^{sc}|^2[\overline{S}(q_z)S_h(q_\parallel,q_z)+\delta S(q_z)S_d(q_\parallel,q_z)]. \tag{1}$$

Here A is the illuminated area on the surface, r_e is the scattering length of the classical electron (2.8×10^{-15} m), and $t_{0,1}^{in}$ and $t_{0,1}^{sc}$ are, in the present approximation, the Fresnel transmission coefficients of the bare water surface for the incident and scattering angles. The first term within brackets in Eq. (1) describes scattering by height fluctuations due to capillary waves. The second term is relevant for heterogeneous films. It describes the noncapillary scattering by domains of the more strongly scattering component (say, a_1) with respect to the other (say, a_2) [27,28]. The average structure factor of this heterogeneous film is given by

$$\overline{S}(q_z)=|[c\tilde{\rho}_{a_1}(q_z)+(1-c)\tilde{\rho}_{a_2}(q_z)]-i\rho_{water}/q_z|^2, \tag{2a}$$

where c the surface coverage of domains of component a_1. Here $\tilde{\rho}_{a_1}(q_z)$ and $\tilde{\rho}_{a_2}(q_z)$ are, respectively, the Fourier transform of the electron densities of the a_1 and a_2 components of the layer and $c\tilde{\rho}_{a_1}(q_z)+(1-c)\tilde{\rho}_{a_2}(q_z)$ is the average electron density of the layer. With $c=0$ or $c=1$, Eq. (1) gives the usual scattering from a film, which is sensitive to both its normal structure through $S(q_z)$ and to the height-height fluctuation spectrum through $S_h(q_\parallel,q_z)$, where all interfaces are assumed to fluctuate conformally. The scattering by height fluctuations for a simple film is given by

$$S_h(q_\parallel,q_z)=e^{-q_z^2\langle\zeta^2\rangle}\int d\mathbf{r}_\parallel(e^{q_z^2C(\mathbf{r}_\parallel)}-1)e^{i\mathbf{q}_\parallel\cdot\mathbf{r}_\parallel}, \tag{2b}$$

where ζ is the interface height and $C(\mathbf{r}_\parallel)=\langle\zeta(\mathbf{0})\zeta(\mathbf{r}_\parallel)\rangle$ is the height-height correlation function whose limiting value for

$r_\parallel \to 0$ is the rms roughness $\sqrt{\langle \zeta^2 \rangle}$. For a heterogeneous film, the noncapillary scattering by domains gives the two additional quantities in the second term of Eq. (1). The relative structure factor of domains of a_1 with respect to a_2 is given by

$$\delta S(q_z) = |\tilde{\rho}_{a_1}(q_z) - \tilde{\rho}_{a_2}(q_z)|^2 \tag{2c}$$

and the domain scattering function by

$$S_d(q_\parallel, q_z) = e^{-q_z^2\langle \zeta^2 \rangle} \int d\mathbf{r}_\parallel e^{q_z^2 C(\mathbf{r}_\parallel)} (P(\mathbf{r}_\parallel) - c^2) e^{i\mathbf{q}_\parallel \cdot \mathbf{r}_\parallel}, \tag{2d}$$

where $p(\mathbf{r}_\parallel)$ is the the probability of finding a domain of a_1 at $r_\parallel$. Generally, $P(\mathbf{r}_\parallel) = \langle p(\mathbf{0}) p(\mathbf{r}_\parallel) \rangle$ will be a function decreasing from c to c^2 over a domain size r_0. We have used $P(\mathbf{r}_\parallel) = c(1-c)\exp(r_\parallel / 2r_0) + c^2$ which has the right dependence. For $c=1$, the correlation function for a liquid surface with surface tension γ and bending rigidity κ is given by [7]

$$C(\mathbf{r}_\parallel) = k_B T/(2\pi\gamma)[K_0(r_\parallel \sqrt{\Delta\rho g/\gamma}) - K_0(r_\parallel \sqrt{\gamma/\kappa})], \tag{3}$$

where k_B is Boltzman's constant, T the absolute temperature, g the acceleration due to gravity, $\Delta\rho$ the density difference across the liquid interface, and K_0 the modified Bessel function of second kind of order 0. The limits of K_0 are $K_0(x)_{x\to 0} \approx \ln 2 - \gamma_E \ln x$ where γ_E is Euler constant, and $K_0(x)_{x\to\infty} = 0$. The correlation function in Eq. (3) adequately describes scattering by capillary waves on various liquid surfaces upto wave vectors ~ 1 nm^{-1} [7,25].

C. Results and discussions

Figure 1 shows the intensity profiles from bare water (open squares), from a stearic acid monolayer on water containing ferric chloride (open triangles) and from a film of preformed ferric stearate on pure water (open circles). It is clear that whereas the acid monolayer behaves exactly as other standard Langmuir monolayers [6,24], the behavior of the preformed fatty-acid salt film is distinctly different, showing much higher diffuse scattering for same surface pressure, $\pi = 20$ mN/m. The most striking features of the scattered intensity from preformed FeSt film at higher surface pressure are (i) an increase of the scattering by two orders of magnitude over the whole q_x range and (ii) appearance of a split peak at around $q_x = 10^8$ m^{-1}. We shall discuss about the dramatic increase of scattering in the relevant subsection and shall concentrate on the peak shape, which relates to a particular structural aspect of the film. $\overline{S(q_z)}$, the average structure factor of the FeSt film in the total scattering function, yields the electron density profile (EDP) along the depth. In particular, the low-q_x part of the scattered intensity, obtained from both the point detector and "PSD," was sensitive to this EDP—i.e., the out-of-plane structure of FeSt on water. The split peak clearly indicates a sandwiched structure more complex than either a simple monolayer with head groups in contact with water as shown in Fig. 1 [inset (a) or (c)] or a layer composed of molecules in the symmetric conformation of Fig. 1 [inset (b)].

Figure 3(a) shows the intensity profiles from bare water (dotted squares), from FeSt film at $\pi = 5$ mN/m (dotted triangles) and from FeSt film at $\pi = 20$ mN/m (dotted circles) with the corresponding fits having the total diffuse scattering function [given by Eq. (1)] represented by dashed, dotted, and solid lines. The EDP obtained from the fit to the data [using Eq. (2a)] is shown in Fig. 3. This EDP can only be reconciled with a model of the FeSt film as a bimolecular

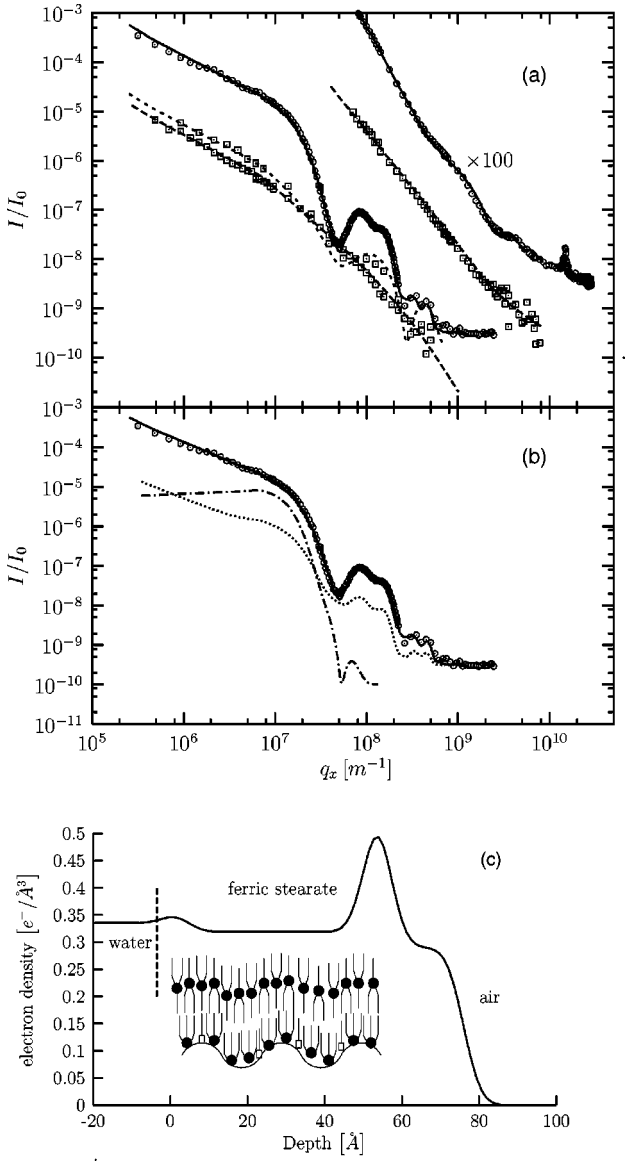

FIG. 3. (a) Scattering from water surface (dotted squares) and ferric stearate films at $\pi = 5mN/m$ (dotted triangles) and at $\pi = 20$ mN/m (dotted circles). The corresponding fits are given by dashed, dotted, and solid lines, respectively. Scattering in the plane of incidence gives the low-$q_\parallel$ scattering whereas scanning around a vertical axis using the PSD and integrating between 2.0 mrad and 12 mrad (multiplied by 100, on the right) gives the large-$q_\parallel$ part. On the same curve, the peak between 10^{10} m^{-1} and 2×10^{10} m^{-1} is due to GID. The scattering from the morphologies observed in AFM is shown in (b). The dotted line is calculated for the scattering of the domains and the dash-dotted line is calculated using a Gaussian correlation function. (c) Electron density of the compressed film. Inset: schematics of the compressed film. Grey circles represent Fe^{3+} and open squares represent free COOH groups.

film on water. In this bimolecular layer, shown in the cartoon of Fig. 3, the bottom layer consists of FeSt molecules in the asymmetric conformation of Fig. 1 [inset (c)] with the Fe-bearing head groups touching water surface, while the top layer has the molecules in the symmetric "Y and inverted-Y" pairs shown in Fig. 1 [inset (b)]. The coexistence of such "symmetric" and "asymmetric" conformations of amphiphilic molecules has been demonstrated in LB films of fatty-acid salts of divalent metals [29,30]. The bottom layer, due to the large dipole moment of the head groups in the asymmetric conformation, couples strongly to the water surface while the top layer has much smaller contribution to the dipole moment of the overall film. This bimolecular combination makes the film stable as well as very dense. It should be noted that this cartoon is only a schematic depiction and the coplanarity of the hydrocarbon chains has not been examined directly. Also the absence of free carboxylic groups in the upper layer could not be established directly, though it is hard to conceive the transfer of such dissociated groups to the upper layer, especially at low surface pressures. The bimolecular model fits the data at all values of surface pressure measured in our experiments (5–20 mN/m), with the thickness of the head group in touch with water decreasing slightly at lower surface pressures. It must be noted here that the scattering profile of FeSt film at 5 mN/m is almost the same as the profile of a stearic acid monolayer over ferric chloride solution at 20 mN/m and both can be explained by a monolayer model given by Fig. 1 [inset (a) or (c)]. The in-plane structure, as obtained from GID, shows a hexagonal packing of untilted chains with in-plane domain size around 6–7 nm and an unit-cell area (area per chain) of around 0.2 nm^2, for all values of surface pressures measured by us.

The most interesting feature of the diffuse scattering profile of FeSt film on water, shown in Fig. 3(a), is the large enhancement, by about two orders of magnitude, of the diffuse scattered intensity as the film is compressed from 5 mN/m to 20 mN/m. We ascribe this difference to enhanced conformal capillary wave height fluctuations at the air-film and film-water interfaces. The only other possible source of large off-specular scattering is the noncapillary scattering from bimolecular domains. To estimate this noncapillary contribution the FeSt films were transferred onto hydrophilic Si substrates at surface pressures of 1 mN/m, 10 mN/m, and 20 mN/m using a horizontal deposition scheme developed by us.

Hydrophilic silicon substrates were kept horizontally in a homemade L-shaped Teflon substrate holder which is attached to the clip of the trough dipper. The substrate holder thus can be moved up and down with desired speed. At the time of film deposition water surface was properly cleaned and the L-shaped substrate holder was immersed into the water so that the substrate was kept parallel to water surface and 10 mm below the air-water interface. Transfer onto Si(001) were done at room temperature, with the substrate moving upwards at the rate of 0.5 mm/min, in this modified inverse Langmuir-Schaefer method [26]. X-ray specular reflectivity data of the transferred films were collected using a rotating anode generator [31].

The reflectivity profile of FeSt film transferred onto a Si(001) surface at $\pi=20$ mN/m is shown (open circles) in Fig. 4 and the fits to the data obtained using standard procedure [31] are shown by the solid line. From the fit the EDP of the FeSt film on the Si(001) surface has been extracted and is shown in the inset of Fig. 4. The EDP clearly indicates a bimolecular layer of FeSt almost identical to the film on water at the same surface pressure [Fig. 3]. This proves again that FeSt films are stable during transfer from water surface to solid surface; in particular, they remain unchanged configurationally during horizontal transfer. FTIR studies of these transferred films show the presence of some COOH groups, obviously due to a small degree of hydrolysis of the head groups, most probably those in contact with water, as indicated in Fig. 3. Again, we cannot say whether some head groups in the upper layer have been dissociated.

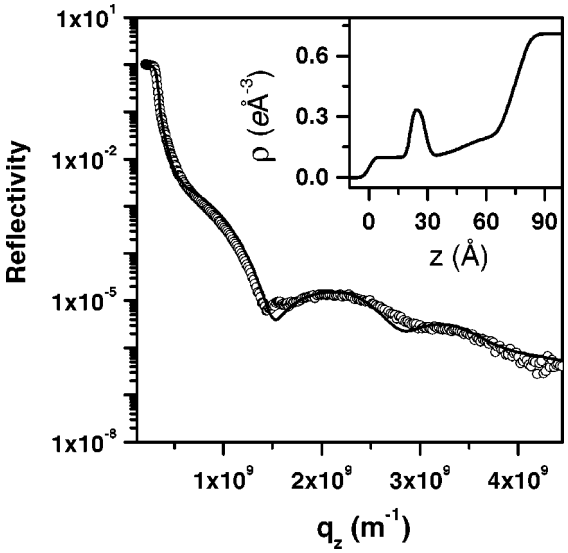

FIG. 4. Reflectivity profile (open circles) of ferric stearate film transferred onto Si(001) surface at $\pi=20$ mN/m by the method described in text. Fit to the data is shown by the solid line. Inset: electron density profile of the film on Si(001) surface extracted from the fit.

Contact-mode AFM data of transferred FeSt films were collected using a Park Scientific Autoprobe CP AFM equipped with a 100-μm scanning head and silicon nitride cantilever (with 0.05-N/m spring constant) and pyramidal tips. The cantilever with lower spring constant value was chosen to minimize damage of the organic films in this mode. Scans were performed over several portions of the film over different scan areas. The film transferred at $\pi=1$ mN/m were found to consist of domains of bimolecular layers coexisting with the monolayer in asymmetric molecular configuration, leading to an overall height fluctuation of $\simeq$1.5 nm and a bimodal distribution in the height histogram [Fig. 5(a)], whereas the film transferred at $\pi=10$ mN/m was found to be homogeneous [Fig. 5(b)], consistent with the EDP of transferred film at higher surface pressure.

Comparison of EDP's on water surface and on Si surface have demonstrated that transferred films are representative of the "frozen" structures at the water surface. Using Eq. (1), we first calculated the scattering profile expected from domains $\simeq$5 nm high and 100 nm is radius as observed in Fig. 5(a). The profile for a rough film on water having the same

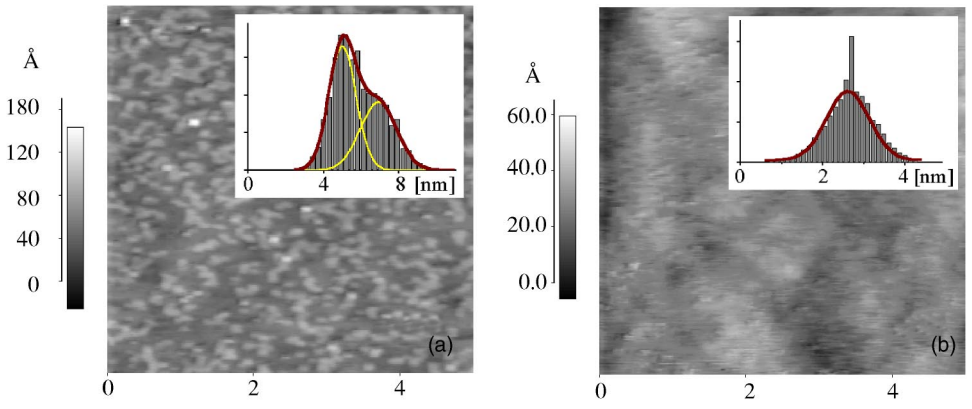

FIG. 5. AFM images ($5 \times 5\ \mu m^2$) of uncompressed (a) and compressed (b) films deposited on silicon wafers. Height histograms for the topographs are shown in corresponding insets. Gaussian fits, also shown, yield for (a) the height maxima at 5.0 nm and 6.9 nm, and the roughness [given by the full width at half maximum (FWHM)] as 1.5 nm and 1.9 nm, respectively. For (b) the maximum is at 2.6 nm and the roughness is 1.0 nm.

height-height correlation as that of a compressed film [Fig. 5(b)] can be modeled as the Gaussian function $\langle \zeta(0)\zeta(\mathbf{r}_\parallel)\rangle = \sigma^2 \exp(r_\parallel^2/2\xi^2)$ with interface width $\sigma = 0.5$ nm and a correlation length $\xi = 0.14\ \mu$m in Eq. (1). These noncapillary contributions to the diffuse scattering were found to be much lower than the observed scattering [Fig. 3(b)]. In particular, they do not exhibit the low-$q_\parallel$ divergence observed in our data, which is characteristic of capillary fluctuations [7], implying that the capillary contributions to the height fluctuations are dominant.

We fitted our diffuse scattering data to Eq. (1) with $c=1$ using the correlation function expected for a liquid surface, given by Eq. (3). This model describes our data very well [Fig. 3(a)] over almost four orders of magnitude with $\gamma = 1.3$ mN/m. For the compressed films γ values ranging from 0.5 mN/m to 5.0 mN/m were found. It is to be noted that the high-$q_\parallel$ scattering from the compressed membrane cannot be accounted for without putting a scattering from small domains (radius $a \approx 1.2$ nm). It has been included in the analysis using a simple form factor for cylindrical domains: $2J_1(q_\parallel a)/(q_\parallel a)$, where J_1 is a Bessel function of the first kind of order 1. It therefore appears that the effective surface tension of the film-covered water surface can be as low as $\simeq 1$ mN/m, more than one order of magnitude below the value ($\simeq 20$ mN/m) obtained with standard surfactants. The fluctuation corresponding to this surface tension comes out to be $\sqrt{\langle \zeta^2 \rangle} \simeq 2.2$ nm.

From the point of view of interfacial energy, the main difference between monolayers at the oil-water and at the air-water interface is an additional surface tension of about 20 mN/m at the air-water interface which is not compensated for by chain repulsion. This repulsion can in principle be increased by compressing the film, but with usual surfactant monolayers, "collapse" generally occurs before very low values of surface tension can be reached. Collapse proceeds by folding or disruption of the film followed by the growth of multilayer domains. This explains why very low values of surface tension are not reached at the air-water interface. The FeSt bimolecular film has two completely different molecular conformations in its two layers. It can, on one hand, couple to the water surface, possibly through the aligned dipoles of the water molecules at the surface [32]. On the other hand, the top layer is expected to have very small dipole moment and serves to increase the chain density and thereby $\pi_\parallel$ without destabilizing the film. Compared to usual monolayers, the processes of folding or rupture leading to collapse will require a much higher energy for this bimolecular layer. A larger decrease in surface tension can therefore be expected on reduction of the area as repulsion ($\pi_\parallel$) can increase to higher values without collapse.

The large scattered intensity at $\pi = 20$ mN/m and the considerable scattered intensity even at $\pi = 5$ mN/m [Fig. 3(a)] both point to a discrepancy between the actual area (A) of the film as measured directly on the trough and the projected area (A_p) covered by the domains, the former being much larger. The height fluctuations must increase for the almost incompressible film to accomodate this discrepancy. This is reminiscent of membranes and would result in an effective Hamiltonian [10], with an effective tension directly linked to the difference between the film area and the projected area fixed here by the Langmuir trough size. If we use the surface spectrum $\langle \zeta(\mathbf{q}_\parallel \zeta) - \mathbf{q}_\parallel \rangle = k_B T/(\Delta\rho g + \gamma q_\parallel^2 + \kappa q_\parallel^4)$ for our height-height correlation function, we find that, with $\delta A = A - A_p$,

$$\delta A/A = k_B T/(8\pi\kappa)\ln[1 + \kappa\Lambda_0^2/\gamma] + C^+ \tag{4a}$$

or

$$\delta A/A \approx k_B T \Lambda_0^2/(8\pi\gamma) + C^+, \tag{4b}$$

where $2\pi/\Lambda_0$ is a molecular cutoff and C^+ is a constant accounting for a possible residual compressibility of the film [10]. Here, γ is not an intrinsic surface tension but the mechanical response to the external constraint fixing A_p. In Fig. 6 we plotted $1/\gamma$ obtained from the x-ray measurements against δA obtained from direct measurement of the trough area assuming that for an incompressible film, the reduction in A_p must be equal to $-\delta A$. As can be seen in Fig. 6, $1/\gamma$ increases linearly with δA in agreement with theory [10].

IV. CONCLUSION

We have shown that ferric stearate, a three-tailed amphiphile, forms a stable bimolecular, rather than a monomolecular, film on a water surface, with molecules in two different conformations in the top and bottom layers. More importantly, we have shown that height fluctuations of the water surface are drastically enhanced in the presence of this bimolecular film. This effect is attributed to the cohesive interactions through the Fe-bearing head groups. The very small resulting surface tension can be interpreted as the me-

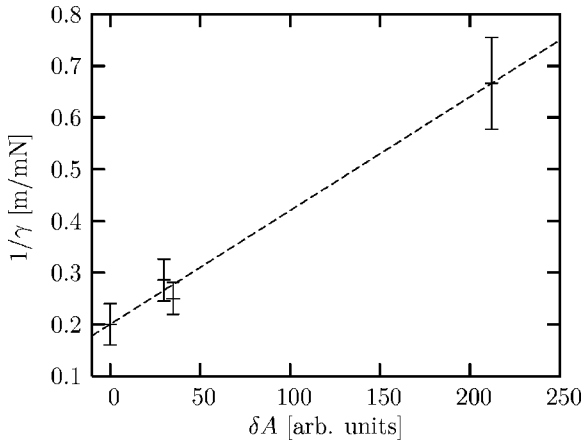

FIG. 6. Inverse of the x-ray determined surface tension as a function of the difference in projected area.

chanical response of the bimolecular film to the constraint of limited available area. We do not know of any independent macroscopic measurement of such drastic reduction in surface tension due to a surface film on water. Such measurements will confirm this effect and are planned to be undertaken by us. These results are expected to be observed with other multivalent ions and, more generally, with any surface layer which do not rupture under compression as usual Langmuir films do. Our work extends the concept of the effective surface tension of membranes to liquid surfaces and therefore represents an important step in the understanding of surface tension, bridging the gap between the better understood fields of membrane tension and intrinsic tension of liquid surfaces.

ACKNOWLEDGMENTS

This work was supported by the Indo-French Centre for Promotion of Advanced Research under Project No. 2504-2. We thank Harald Mueller of ESRF for the initial FTIR spectra, Sudipta Pal of SINP for her help in Atomic Force Microscopy, and J.B. Fournier for useful discussions.

[1] J. S. Rowlinson and B. Widom, *Molecular Theory of Capillarity*, Vol. 8 of The International Series of Monographs on Chemistry (Oxford University Press, Oxford, 1982).
[2] G. Gompper and M. Schick, in *Phase Transitions and Critical Phenomena* (Academic Press, New York, 1994).
[3] H. Leitao, M. M. Telo da Gama, and R. Strey, J. Chem. Phys. **108**, 4189 (1998).
[4] V. A. Parsegian, Trans. Faraday Soc. **62**, 848 (1966).
[5] A. Braslau, M. Deutsch, P. S. Pershan, A. H. Weiss, J. Als-Nielsen, and J. Bohr, Phys. Rev. Lett. **54**, 114 (1985).
[6] J. Daillant, L. Bosio, J. J. Benattar, and J. Meunier, Europhys. Lett. **8**, 453 (1989).
[7] M. K. Sanyal, S. K. Sinha, K. G. Huang, and B. M. Ocko, Phys. Rev. Lett. **66**, 628 (1991).
[8] C. Fradin, A. Braslau, D. Luzet, D. Smilgies, M. Alba, N. Boudet, K. Mecke, and J. Daillant, Nature (London) **403**, 871 (2000).
[9] W. Helfrich and R.-M. Servuss, Nuovo Cimento D **3**, 137 (1984).
[10] J.-B. Fournier, A. Ajdari, and L. Peliti, Phys. Rev. Lett. **86**, 4970 (2001).
[11] O. Farago and P. Pincus, Eur. Phys. J. E **11**, 399 (2004).
[12] E. Evans and W. Rawicz, Phys. Rev. Lett. **64**, 2094 (1990).
[13] S. K. Sinha, E. B. Sirota, S. Garoff, and H. B. Stanley Phys. Rev. B **38**, 2297 (1988).
[14] J. Daillant and M. Alba, Rep. Prog. Phys. **63**, 1725 (2000).
[15] C. Fradin, A. Braslau, D. Luzet, M. Alba, C. Gourier, J. Daillant, G. Grubel, G. Vignaud, J. F. Legrand, J. Lal, J. M. Petit, and F. Rieutord, Physica B **248**, 310 (1998).
[16] J. Kmetko, A. Datta, G. Evmenenko, and P. Dutta, J. Phys. Chem. B **105**, 10818, (2001).
[17] I. Weissbuch, S. Guo, R. Edgar, S. Cohen, P. Howes, K. Kjaer, J. Als-Nielsen, M. Lahav, and L. Leiserowitz, Adv. Mater. (Weinheim, Ger.) **10**, 117 (1998).
[18] M. Prakash, J. B. Peng, J. B. Ketterson, and P. Dutta, Thin Solid Films **146**, L15 (1987).
[19] A. Datta, M. K. Sanyal, A. Dhanabalan, and S. S. Major, J. Phys. Chem. B **101**, 9780 (1997).
[20] D. Sarkar, A. Paul, and T. N. Misra, Thin Solid Films **227**, 105 (1993).
[21] A. Brugger, Ch. Schoppmann, M. Schurr, M. Seidl, G. Sipos, C. Y. Hann, J. Hassmann, O. Waldmann, and H. Voit, Thin Solid Films **338**, 231 (1999).
[22] W. Meisel, P. Tippmann-Krayer, H. Möhwald, and P. Gütlich, Fresenius' J. Anal. Chem. **341**, 289 (1991).
[23] M. K. Sanyal, J. K. Basu, and A. Datta, Physica B **248**, 217 (1998).
[24] C. Fradin, J. Daillant, A. Braslau, D. Luzet, M. Alba, and M. Goldmann, Eur. Phys. J. B **1**, 57 (1998).
[25] S. Mora, J. Daillant, K. Mecke, D. Luzet, A. Braslau, M. Alba, and B. Struth, Phys. Rev. Lett. **90**, 216101 (2003).
[26] K. Y. C. Lee, M. M. Lipp, D. Y. Takamoto, E. Ter-Ovanesyan, and J. A. Zasadzinski, Langmuir **14**, 2567 (1998).
[27] M. Fukuto, R. K. Heilmann, P. S. Pershan, J. A. Griffiths, S. M. Yu, and D. A. Tirrell, Phys. Rev. Lett. **81**, 3455 (1998).
[28] M. Li, A. M. Tikhonov, and M. L. Schlossman, Europhys. Lett. **58**, 80 (2002).
[29] A. Malik, M. K. Durbin, A. G. Richter, K. G. Huang, and P. Dutta, Phys. Rev. B **52**, R11654 (1995).
[30] M. K. Sanyal, M. K. Mukhopadhyay, M. Mukherjee, A. Datta, J. K. Basu, and J. Penfold, Phys. Rev. B **65**, 033409 (2002).
[31] J. K. Basu and M. K. Sanyal, Phys. Rep. **363**, 1 (2002).
[32] D. E. Gragson, and G. L. Richmond, J. Phys. Chem. B **102**, 3847 (1998).